GEOPHYSICS, VOL. 83, NO. 1 (JANUARY-FEBRUARY 2018); P. C1–C11, 12 FIGS.
10.1190/GEO2016-0638.1

Approximate reflection coefficients for a thin VTI layer

Qi Hao[1] and Alexey Stovas[2]

ABSTRACT

We have developed an approximate method to derive simple expressions for the reflection coefficients of P- and SV-waves for a thin transversely isotropic layer with a vertical symmetry axis (VTI) embedded in a homogeneous VTI background. The layer thickness is assumed to be much smaller than the wavelengths of P- and SV-waves inside. The exact reflection and transmission coefficients are derived by the propagator matrix method. In the case of normal incidence, the exact reflection and transmission coefficients are expressed in terms of the impedances of vertically propagating P- and S-waves. For subcritical incidence, the approximate reflection coefficients are expressed in terms of the contrast in the VTI parameters between the layer and the background. Numerical examples are designed to analyze the reflection coefficients at normal and oblique incidence and investigate the influence of transverse isotropy on the reflection coefficients. Despite giving numerical errors, the approximate formulas are sufficiently simple to qualitatively analyze the variation of the reflection coefficients with the angle of incidence.

INTRODUCTION

Reflection and transmission coefficients of plane waves are of importance in studying wave propagation. In reflection seismology, the main application of reflection coefficient studies is to analyze the amplitude variation with offset (AVO). Parameters of reservoir rocks such as fluid content, density, and seismic wave velocities may be determined from the variation of amplitude with incidence angle and azimuth.

For an interface separating two elastic half-spaces, the exact plane-wave reflection and transmission coefficients can be derived from the boundary condition that displacement and traction are continuous across the interface (Aki and Richards, 2002). Although it is straightforward to numerically calculate the reflection and transmission coefficients, the exact formulas suffer from high algebraic complexity. Simple approximate formulas help to analyze the influence of the changes in the medium parameters across the interface on the reflection and transmission coefficients. For isotropic and anisotropic media, these approximate formulas can be found, for example, in Aki and Richards (2002), Thomsen (1993), Rüger (1996, 1997, 1998), Ursin and Haugen (1996), Vavryčuk and Pšenčík (1998), and Vavryčuk (1999). These approximations assume a weak contrast in density and velocity parameters, and weak anisotropy for a specific parameterization of the considered medium.

For horizontally layered elastic models, reflection and transmission of plane waves can be described by the propagator matrix method. For a single horizontal layer, the propagator matrix is constructed by considering the continuity of the particle displacement and traction at the top and bottom of the layer. For horizontally layered media, the whole propagator matrix linking the displacement and traction at the top to those at the bottom is represented by the product of the individual propagator matrices. The propagator matrix method to calculate reflection and transmission coefficients is systematically discussed in the monographs by Brekhovskikh (1980), Kennett (1983), Brekhovskikh and Godin (1989), Nayfeh (1995), and Chapman (2004). The propagator matrix method for anisotropic media can be found in Fryer and Frazer (1984, 1987). More literature related to the propagator matrix method is referenced in these monographs.

In this paper, we study the reflection and transmission of plane waves from a thin homogeneous transversely isotropic layer with a vertical symmetry axis (VTI) embedded in a homogeneous VTI background (Figure 1). The term "thin" means that the thickness of the layer is much smaller than the wavelengths of the waves

This paper is based on the expanded abstract that was presented at the 17th International Workshop on Seismic Anisotropy, September 18–23, 2016, in Austin, Texas, USA. Manuscript received by the Editor 1 December 2016; revised manuscript received 22 August 2017; published ahead of production 17 September 2017; published online 13 November 2017.
[1]Formerly Norwegian University of Science and Technology (NTNU), Trondheim, Norway; presently King Abdullah University of Science and Technology (KAUST), Thuwal, Saudi Arabia. E-mail: xqi.hao@gmail.com.
[2]Norwegian University of Science and Technology (NTNU), Trondheim, Norway. E-mail: alexey.stovas@ntnu.no.

propagating inside it. We consider the cases of P- and SV-wave incidence from the upper half-space. In addition to the Voigt notation, Thomsen's (1986) notation is used to describe a VTI medium. In Thomsen's (1986) notation, v_{P0} and v_{S0} denote the velocities of the vertically propagating P- and S-waves; ε and δ denote Thomsen's (1986) anisotropy parameters. The density of the medium is denoted by ρ. The stiffness coefficients can be explicitly expressed in terms of Thomsen's parameters and density. For brevity, the term "plane" is omitted when describing P- and SV-waves throughout this paper.

The rest of the paper is organized as follows: First, we introduce the exact and approximate propagator matrices for a horizontal homogeneous VTI layer. Then, we present equations for the reflection and transmission coefficients for a layer embedded in a homogeneous VTI background. Next, we introduce specific assumptions for the parameters of the layer and background, and we derive relatively simple formulas for the reflection and transmission coefficients. Finally, we implement the proposed formulas to analyze the reflection and transmission coefficients for several VTI models.

PROPAGATOR MATRIX FOR A SINGLE VTI LAYER

The horizontal slowness component is preserved for the incident, reflected, and transmitted waves in a horizontal layer (Figure 1). For all these waves, the unit polarization vector and the vertical slowness can be expressed in terms of the horizontal slowness component. The particle displacement and the traction are continuous across the upper and lower interfaces of the layer. The particle velocity, as the first-order derivative of particle displacement with respect to time, is also continuous across these interfaces. The particle velocity and the traction at the upper interface are linked to those at the lower interface by the propagator matrix B_{ij} (Appendix A)

$$\begin{pmatrix} v_x \\ v_z \\ \tau_{zz} \\ \tau_{zx} \end{pmatrix}\Bigg|_{z=0} = \begin{pmatrix} B_{11} & B_{12} & B_{13} & B_{14} \\ B_{21} & B_{22} & B_{23} & B_{24} \\ B_{31} & B_{32} & B_{33} & B_{34} \\ B_{41} & B_{42} & B_{43} & B_{44} \end{pmatrix} \begin{pmatrix} v_x \\ v_z \\ \tau_{zz} \\ \tau_{zx} \end{pmatrix}\Bigg|_{z=h}, \tag{1}$$

where B_{ij} are the functions of the horizontal slowness component (explicit expressions for B_{ij} are given in equations A-9–A-18 in Appendix A), v_x and v_z are the horizontal and vertical components of the particle velocity, τ_{zx} and τ_{zz} denotes two components of a stress tensor, and $z = 0$ and $z = h$ correspond to the top and bottom of the layer.

Equation 1 plays the role of the boundary condition, which is used to link the incident and reflected waves in the upper half-space to the transmitted waves in the lower half-space. As illustrated in equations A-9–A-18 in Appendix A, the layer thickness h appears in B_{ij} in the dimensionless terms $hq_P\omega$ and $hq_S\omega$, where q_P and q_S denote the vertical slowness components of the P- and SV-waves, respectively. If the layer thickness is much smaller than the wavelengths of the P- and SV-waves propagating inside this layer, then $hq_P\omega < hq_S\omega \ll 1$. We expand equation 1 in $hq_P\omega$ and $hq_S\omega$, and we then further expand q_P and q_S in the horizontal slowness p. The final expression is truncated after the quadratic terms in h

$$\begin{pmatrix} B_{11} & B_{12} & B_{13} & B_{14} \\ B_{21} & B_{22} & B_{23} & B_{24} \\ B_{31} & B_{32} & B_{33} & B_{34} \\ B_{41} & B_{42} & B_{43} & B_{44} \end{pmatrix} \approx \begin{pmatrix} 1 & 0 & 0 & 0 \\ 0 & 1 & 0 & 0 \\ 0 & 0 & 1 & 0 \\ 0 & 0 & 0 & 1 \end{pmatrix}$$
$$+ ih\omega \begin{pmatrix} 0 & B_{12}^{(1)} & 0 & B_{14}^{(1)} \\ B_{21}^{(1)} & 0 & B_{23}^{(1)} & 0 \\ 0 & B_{32}^{(1)} & 0 & B_{34}^{(1)} \\ B_{41}^{(1)} & 0 & B_{43}^{(1)} & 0 \end{pmatrix} - h^2\omega^2 \begin{pmatrix} B_{11}^{(2)} & 0 & B_{13}^{(2)} & 0 \\ 0 & B_{22}^{(2)} & 0 & B_{24}^{(2)} \\ B_{31}^{(2)} & 0 & B_{33}^{(2)} & 0 \\ 0 & B_{42}^{(2)} & 0 & B_{44}^{(2)} \end{pmatrix}, \tag{2}$$

where i denotes the imaginary unity, ω denotes the angular frequency, and the nonzero elements $B_{ij}^{(1)}$ and $B_{ij}^{(2)}$ are given by equations A-21–A-30.

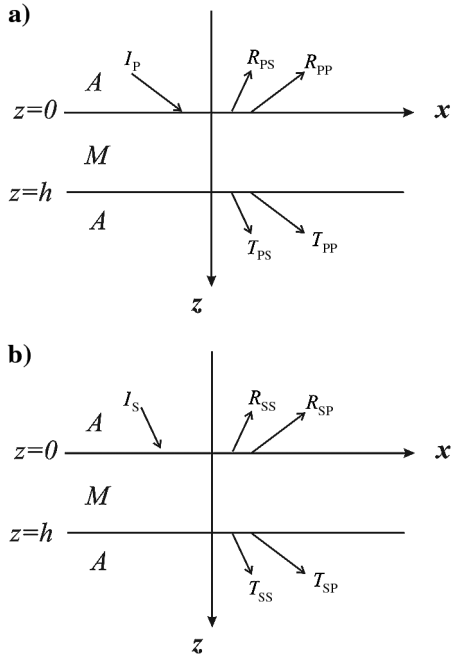

Figure 1. Schematic plots for plane-wave reflection and transmission from a single VTI layer: (a) P-wave incidence and (b) SV-wave incidence. The waves propagate in the $[x, z]$ plane of a Cartesian coordinate system. The symbol A denotes the homogeneous VTI background, and M denotes the layer. (a) The symbols I_P, R_{PP}, R_{PS}, T_{PP}, and T_{PS} denote the incident P-wave, the P-P reflected wave, the P-SV reflected wave, the P-P transmitted wave, and the P-SV transmitted wave, respectively. (b)The symbols I_S, R_{SP}, R_{SS}, T_{SP}, and T_{SS} denote the incident SV-wave, the SV-P reflected wave, the SV-SV reflected wave, the SV-P transmitted wave, and the SV-SV transmitted wave, respectively.

EXACT REFLECTION AND TRANSMISSION COEFFICIENTS

As illustrated in Figure 1, we consider the reflection and transmission for P- and SV-waves separately incident upon the top of the layer. For the incident, reflected, and transmitted P- and SV-waves,

the horizontal component of the polarization unit vector is chosen to be always nonnegative, which agrees with the convention in Aki and Richards (2002).

P-wave incidence

Referring to Figure 1a, the particle displacement functions of the incident, reflected, and transmitted waves are defined as follows in terms of the horizontal slowness component:

- incident P-wave

$$\mathbf{u}_{\mathrm{P}\downarrow}^{(A-)} = (l_{\mathrm{P}}, 0, m_{\mathrm{P}})^T \exp(-i\omega(t - px - q_{\mathrm{P}}z)), \quad z \in (-\infty, 0) \tag{3}$$

- reflected P-wave

$$\mathbf{u}_{\mathrm{P}\uparrow}^{(A-)} = R_{\mathrm{PP}}(l_{\mathrm{P}}, 0, -m_{\mathrm{P}})^T \exp(-i\omega(t - px + q_{\mathrm{P}}z)), \quad z \in (-\infty, 0) \tag{4}$$

- reflected SV-wave

$$\mathbf{u}_{\mathrm{S}\uparrow}^{(A-)} = R_{\mathrm{PS}}(l_{\mathrm{S}}, 0, m_{\mathrm{S}})^T \exp(-i\omega(t - px + q_{\mathrm{S}}z)), \quad z \in (-\infty, 0) \tag{5}$$

- transmitted P-wave

$$\mathbf{u}_{\mathrm{P}\downarrow}^{(A+)} = T_{\mathrm{PP}}(l_{\mathrm{P}}, 0, m_{\mathrm{P}})^T \exp(-i\omega(t - px - q_{\mathrm{P}}z)), \quad z \in (h, +\infty) \tag{6}$$

- transmitted SV-wave

$$\mathbf{u}_{\mathrm{S}\downarrow}^{(A+)} = T_{\mathrm{PS}}(l_{\mathrm{S}}, 0, -m_{\mathrm{S}})^T \exp(-i\omega(t - px - q_{\mathrm{S}}z)), \quad z \in (h, +\infty), \tag{7}$$

where $\mathbf{u}$ denotes the vector of particle displacement, the superscripts $A-$ and $A+$ denote the upper $(A-)$ and lower $(A+)$ half-spaces relative to the layer, T denotes the transpose of a vector, the subscripts P and S denote P- and SV-waves, the arrows $\downarrow$ and $\uparrow$ in the subscripts denote upgoing and downgoing waves, l and m denote the absolute values of the horizontal and vertical components of the unit polarization vector of a considered wave, p denotes the horizontal slowness component, and q_{P} and q_{S} denote the magnitudes of the vertical slowness components of the P- and SV-waves. Explicit expressions for the polarization and slowness components can be found in Rüger (1996); R_{PP} and R_{PS} denote the P-P and P-SV reflection coefficients, and T_{PP} and T_{PS} denote the P-P and P-SV transmission coefficients, where the first subscript denotes the incident wave and the second subscript denotes the reflected or transmitted wave; i is the imaginary unity; and t and ω denote the time and angular frequency, x and z denote the horizontal and vertical coordinates, and h denotes the layer thickness.

SV-wave incidence

As illustrated in Figure 1b, we consider the SV-wave incident from the upper half-space. By analogy with the definitions in equations 3–7, the particle displacement functions of the incident, reflected, and transmitted waves are found as follows:

- incident SV-wave

$$\mathbf{u}_{\mathrm{S}\downarrow}^{(A-)} = (l_{\mathrm{S}}, 0, -m_{\mathrm{S}})^T \exp(-i\omega(t - px - q_{\mathrm{S}}z)), \quad z \in (-\infty, 0) \tag{8}$$

- reflected P-wave

$$\mathbf{u}_{\mathrm{P}\uparrow}^{(A-)} = R_{\mathrm{SP}}(l_{\mathrm{P}}, 0, -m_{\mathrm{P}})^T \exp(-i\omega(t - px + q_{\mathrm{P}}z)), \quad z \in (-\infty, 0) \tag{9}$$

- reflected SV-wave

$$\mathbf{u}_{\mathrm{S}\uparrow}^{(A-)} = R_{\mathrm{SS}}(l_{\mathrm{S}}, 0, m_{\mathrm{S}})^T \exp(-i\omega(t - px + q_{\mathrm{S}}z)), \quad z \in (-\infty, 0) \tag{10}$$

- transmitted P-wave

$$\mathbf{u}_{\mathrm{P}\downarrow}^{(A+)} = T_{\mathrm{SP}}(l_{\mathrm{P}}, 0, m_{\mathrm{P}})^T \exp(-i\omega(t - px - q_{\mathrm{P}}z)), \quad z \in (h, +\infty) \tag{11}$$

- transmitted SV-wave

$$u_{\mathrm{S}\downarrow}^{(A+)} = T_{\mathrm{SS}}(l_{\mathrm{S}}, 0, -m_{\mathrm{S}})^T \exp(-i\omega(t - px - q_{\mathrm{S}}z)), \quad z \in (h, +\infty), \tag{12}$$

where R_{SP} and R_{SS} denote the SV-P and SV-SV reflection coefficients and T_{SP} and T_{SS} denote the corresponding transmission coefficients.

Equations for reflection and transmission coefficients

Using the displacement functions 3–7, we can obtain the particle velocity and traction in the upper and lower half-spaces. The substitution of the particle velocity and traction into equation 1 allows us to derive a system of equations for the reflection and transmission coefficients for an incident P-wave. Similarly, we may also obtain another system of equations for the reflection and transmission coefficients in the case of SV-wave incidence. After combining the two systems, we obtain the following system of equations for the reflection and transmission coefficients:

$$\begin{pmatrix} l_{\mathrm{P}} & l_{\mathrm{S}} & E_1 & F_1 \\ -m_{\mathrm{P}} & m_{\mathrm{S}} & E_2 & F_2 \\ -c_{\mathrm{P}} & -d_{\mathrm{S}} & E_3 & F_3 \\ a_{\mathrm{P}} & b_{\mathrm{S}} & E_4 & F_4 \end{pmatrix} \begin{pmatrix} R_{\mathrm{PP}} & R_{\mathrm{SP}} \\ R_{\mathrm{PS}} & R_{\mathrm{SS}} \\ T_{\mathrm{PP}} & T_{\mathrm{SP}} \\ T_{\mathrm{PS}} & T_{\mathrm{SS}} \end{pmatrix} = \begin{pmatrix} -l_{\mathrm{P}} & -l_{\mathrm{S}} \\ -m_{\mathrm{P}} & m_{\mathrm{S}} \\ c_{\mathrm{P}} & d_{\mathrm{S}} \\ a_{\mathrm{P}} & b_{\mathrm{S}} \end{pmatrix}, \tag{13}$$

with

$$a_P = c_{55}(q_P l_P + p m_P), \tag{14}$$

$$b_S = c_{55}(q_S l_S - p m_S), \tag{15}$$

$$c_P = c_{13} p l_P + c_{33} q_P m_P, \tag{16}$$

$$d_S = c_{13} p l_S - c_{33} q_S m_S, \tag{17}$$

$$E_i = (B_{i4} a_P + B_{i3} c_P - B_{i1} l_P - B_{i2} m_P) \exp(i\omega q_P h), \tag{18}$$

$$F_i = (B_{i4} b_S + B_{i3} d_S - B_{i1} l_S + B_{i2} m_S) \exp(i\omega q_S h), \tag{19}$$

where B_{ij} correspond to the layer, whereas the other quantities including the stiffness coefficients c_{11}, c_{13}, c_{33}, and c_{55}, the absolute values l and m of the components of the polarization vector, and the vertical slowness component q, correspond to the upper and lower half-spaces. Equation 13 describes the exact reflection and transmission coefficients for a homogeneous, horizontal VTI layer embedded in a homogeneous VTI background.

In the case of normal incidence, the horizontal slowness vanishes, and the reflection and transmission coefficients are given by

$$R_{PP} = \frac{2 r_{P0} \sin k_{P0}^{(M)}}{(1 + r_{P0}^2) \sin k_{P0}^{(M)} + i(1 - r_{PP}^2) \cos k_{P0}^{(M)}}, \tag{20}$$

$$R_{SS} = \frac{2 r_{S0} \sin k_{S0}^{(M)}}{(1 + r_{S0}^2) \sin k_{S0}^{(M)} + i(1 - r_{S0}^2) \cos k_{S0}^{(M)}}, \tag{21}$$

$$T_{PP} = \frac{1 - r_{P0}^2}{(1 - r_{P0}^2) \cos k_{P0}^{(M)} - i(1 + r_{P0}^2) \sin k_{P0}^{(M)}}, \tag{22}$$

$$T_{SS} = \frac{1 - r_{S0}^2}{(1 - r_{S0}^2) \cos k_{S0}^{(M)} - i(1 + r_{S0}^2) \sin k_{S0}^{(M)}}, \tag{23}$$

with

$$r_{P0} = \frac{Z_{P0}^{(M)} - Z_{P0}^{(A)}}{Z_{P0}^{(M)} + Z_{P0}^{(A)}}, \qquad r_{S0} = \frac{Z_{S0}^{(M)} - Z_{S0}^{(A)}}{Z_{S0}^{(M)} + Z_{S0}^{(A)}}, \tag{24}$$

$$k_{P0}^{(M)} = \frac{h\omega}{v_{P0}^{(M)}}, \qquad k_{S0}^{(M)} = \frac{h\omega}{v_{S0}^{(M)}}, \tag{25}$$

where $Z_{P0} = \rho v_{P0}$ and $Z_{S0} = \rho v_{S0}$ denote the impedances of the vertically propagating P- and S-waves and the superscripts M and A denote the layer and the background, respectively.

APPROXIMATE REFLECTION AND TRANSMISSION COEFFICIENTS

By analogy with the weak-contrast, weak-anisotropy approximations for the reflection and transmission coefficients at an interface separating two VTI half-spaces (Thomsen, 1993), we make the following assumptions to derive approximate formulas for the reflection coefficients from a thin layer.

First, we assume a small contrast in the elastic properties (including the density ρ, the P-wave vertical velocity v_{P0}, and the S-wave vertical velocity v_{S0}) at the top and bottom of the layer

$$\left|\frac{\Delta v_{P0}}{\bar{v}_{S0}}\right| \ll 1, \quad \left|\frac{\Delta v_{S0}}{\bar{v}_{S0}}\right| \ll 1, \quad \left|\frac{\Delta \rho}{\bar{\rho}}\right| \ll 1, \tag{26}$$

where $\Delta\alpha = \alpha^{(M)} - \alpha^{(A)}$, and $\bar{\alpha} = (\alpha^{(M)} + \alpha^{(A)})/2$ denote the difference and the average of the medium parameters α in the layer (corresponding to the superscript M) and background (corresponding to the superscript A).

Second, we assume weak anisotropy for the layer and background:

$$|\varepsilon^{(\mu)}| \ll 1, \qquad |\delta^{(\mu)}| \ll 1, \tag{27}$$

where the superscript μ is taken as M and A for the layer and background, respectively.

Finally, the VTI layer is assumed to be so thin that it satisfies the following inequality:

$$h q_P^{(M)} \omega < h q_s^{(M)} \omega \ll 1, \tag{28}$$

where $q_P^{(M)}$ and $q_S^{(M)}$ denote the vertical slowness components of the P- and SV-waves, respectively, in the layer and are functions of the horizontal slowness component.

We start with equation 13 for the reflection and transmission coefficients, where the propagator matrix B_{ij} is approximated by equation 2. The exponential functions in equations 18 and 19 are expanded with respect to $hq_P\omega$ and $hq_S\omega$, and then q_P and q_S are expanded with respect to the horizontal slowness component. The horizontal slowness component is expressed in terms of incidence angles θ_P and θ_S for the P- and SV-waves, respectively. The density and velocity parameters of the background medium and the layer are expressed in terms of their averages and differences. These operations allow us to expand the exact reflection coefficients with respect to the contrasts in the density, the velocities of vertically propagating P- and S-waves, Thomsen's anisotropy parameters, and the layer thicknesses normalized by the velocities of the vertically propagating P- and S-waves. We also consider the expansion of the reflection coefficients with respect to the sine of the incident angles to obtain simple expressions for the approximate reflection coefficients. As a result, the approximate reflection coefficients are as follows:

- P-P-wave reflection coefficient

$$R_{PP} \approx |r_{PP}| \exp(i\phi_{PP}), \tag{29}$$

with

$$r_{PP} = \omega h(a_{PP} + b_{PP} \sin^2 \theta_P), \tag{30}$$

$$\phi_{PP} = \frac{\pi}{2} \text{sign}(r_{PP}) + \tan^{-1}\left(\frac{\omega h}{\bar{v}_{P0}} \cos(\theta_P)\right), \tag{31}$$

where θ_P denotes the angle of incidence of P-waves, and explicit expressions for a_{PP} and b_{PP} are given in equations B-1 and B-2 of Appendix B.

P-SV reflection coefficient

$$R_{PS} \approx |r_{PS}| \exp(i\phi_{PS}), \tag{32}$$

with

$$r_{PS} = \omega h \sin \theta_P (a_{PS} + b_{PS} \sin^2 \theta_P), \tag{33}$$

$$\phi_{PS} = \frac{\pi}{2} \text{sign}(r_{PS}) + \tan^{-1}\left(\omega h \frac{c_{PS} + d_{PS} \sin^2 \theta_P}{a_{PS} + b_{PS} \sin^2 \theta_P}\right), \tag{34}$$

where explicit expressions for a_{PS}, b_{PS}, c_{PS}, and d_{PS} are given in equations B-3–B-6 of Appendix B.

SV-SV reflection coefficient

$$R_{SS} \approx |r_{SS}| \exp(i\phi_{SS}), \tag{35}$$

with

$$r_{SS} = \omega h(a_{SS} + b_{SS} \sin^2 \theta_S), \tag{36}$$

$$\phi_{SS} = \frac{\pi}{2} \text{sign}(r_{SS}) + \tan^{-1}\left(\frac{\omega h}{\bar{v}_{S0}} \cos(\theta_S)\right), \tag{37}$$

where θ_S denotes the angle of incidence of SV-waves, and explicit expressions for a_{SS} and b_{SS} are given in equations B-7 and B-8 of Appendix B.

SV-P reflection coefficient

$$R_{SP} \approx |r_{SP}| \exp(i\phi_{SP}), \tag{38}$$

with

$$r_{SP} = \omega h \sin \theta_S (a_{SP} + b_{SP} \sin^2 \theta_S), \tag{39}$$

$$\phi_{SP} = \frac{\pi}{2} \text{sign}(r_{SP}) + \tan^{-1}\left(\omega h \frac{c_{SP} + d_{SP} \sin^2 \theta_S}{a_{SP} + b_{SP} \sin^2 \theta_S}\right), \tag{40}$$

where $a_{SP} = a_{PS}$, and explicit expressions for a_{PS}, b_{PS}, c_{PS}, and d_{PS} are given in equations B-9–B-12 of Appendix B.

In equations 30 and 36, the coefficients a_{PP} and a_{SS} determine the magnitudes of the P-P and SV-SV reflection coefficients at normal incidence, and the coefficients b_{PP} and b_{SS} govern the curvatures of the reflection-coefficient magnitudes with respect to the incidence angles. In equations 33 and 39, the coefficients a_{PS} and a_{SP} describe the gradients of the magnitudes of the P-SV- and SV-P-wave reflection coefficients with respect to the corresponding incidence angles and the coefficients b_{PS} and b_{SP} describe the higher order terms with respect to θ_P and θ_S. For small incidence angles, the converted-wave reflection coefficients are mostly controlled by the coefficients a_{PS} and a_{SP}.

Referring to equations in Appendix B, the approximate reflection coefficients indicate that (1) the reflection coefficients vanish when the layer thickness tends to zero because the medium properties above and below the layer are identical; (2) the magnitude of the reflection coefficients increases with frequency, albeit just for the limited frequency range in which the layer remains thin compared with the predominant wavelength; (3) the curvatures of the magnitudes of the P-P and SV-SV wave reflection coefficients with respect to the incidence angles are controlled by the changes in the anisotropy parameters δ and σ across the layer boundaries (σ is the combination of Thomsen's parameters, defined after equation B-6); (4) the gradient and torsion of the magnitude of the P-SV-wave reflection coefficient with respect to the incidence angle depend on the changes in δ and σ (respectively) across the layer boundaries; (5) the gradient of the magnitude of the SV-P-wave reflection coefficient with respect to the incidence angle is identical to that of the P-SV-wave reflection coefficient; and (6) the torsion of the magnitude of the SV-P-wave reflection coefficient with respect to the incidence angle involves the changes in ε and δ across the layer boundaries and cannot be described in terms of the single parameter σ.

NUMERICAL EXAMPLES

We use two single-layer models (Figure 1) to investigate the reflection coefficients of the incident P- and SV-waves. The first model includes a high-velocity thin VTI layer embedded in a homogeneous isotropic background. The second model includes a low-velocity thin VTI layer embedded in the same isotropic background. The second model is obtained by reducing the layer velocities $v_{P0}^{(M)}$ and $v_{S0}^{(M)}$ from the first model, whereas all other parameters remain the same.

In the first example, we investigate the influence of wavelength on the P-P- and S-S-wave normal-incidence reflection coefficients (equations 20 and 21). Figures 2 and 3 show that those coefficients are periodic functions of wavelength. A comparison of Figures 2 and 3 shows that the magnitudes of the P-P and S-S reflection coefficients for the high- and low-velocity layers are similar, whereas the phases are different. When the layer thickness is much smaller than the wavelengths of the vertically propagating P- and S-waves inside the

layer (i.e., $h/\lambda_{P0} \le 0.2$ and $h/\lambda_{S0} \le 0.2$), the magnitudes of the reflection coefficients have a sinusoidal shape, and the phases increase linearly with the normalized layer thickness.

Next, we investigate the influence of the anisotropy parameters on the reflection coefficients. The coefficients b_{PP} and b_{SS} determine the curvatures of the magnitudes of the P-P- and SV-SV-wave reflection coefficients with respect to the incidence angles. Figures 4 and 5 show that b_{PP} and b_{SS} vary linearly with the changes in δ and σ (respectively) across the layer boundaries. A comparison of Figures 6 and 7 indicates that the coefficients a_{PS} and b_{PS}, which determine the gradient and torsion of the magnitude of the P-SV-wave reflection coefficients, also have a linear dependence on the changes in δ and σ (respectively) across the layer boundaries. The coefficients a_{SP} and b_{SP} control the magnitude of the P-SV-wave reflection coefficients. The coefficient a_{SP} is identical to a_{PS} (equation B-9), whereas the coefficient b_{SP} (equation B-10) cannot be expressed in terms of the change in the single parameter σ, as discussed above. Figure 8

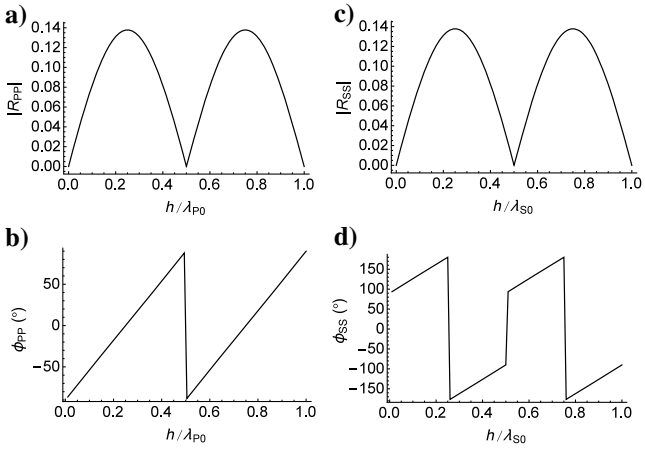

Figure 2. P-P- and S-S-wave normal-incidence reflection coefficients for the high-velocity VTI layer as a function of the layer thickness normalized by the wavelength. (a b) The magnitude and phase of the P-P-wave reflection coefficient. (c d) The magnitude and phase of the S-S-wave reflection coefficient. The symbols λ_{P0} and λ_{S0} denote the wavelengths of the vertically propagating P- and S-waves inside the layer, respectively, and h is the layer thickness. The parameters of the isotropic background include $v_{P0}^{(A)} = 3.0$ km/s, $v_{S0}^{(A)} = 1.5$ km/s, and $\rho^{(A)} = 2.6$ g/cm^3, and the parameters of the VTI layer include $v_{P0}^{(M)} = 3.2$ km/s, $v_{S0}^{(M)} = 1.6$ km/s, $\rho^{(M)} = 2.8$ g/cm^3, $\varepsilon^{(M)} = 0.1$, $\delta^{(M)} = 0.2$, and $h = 15$ m.

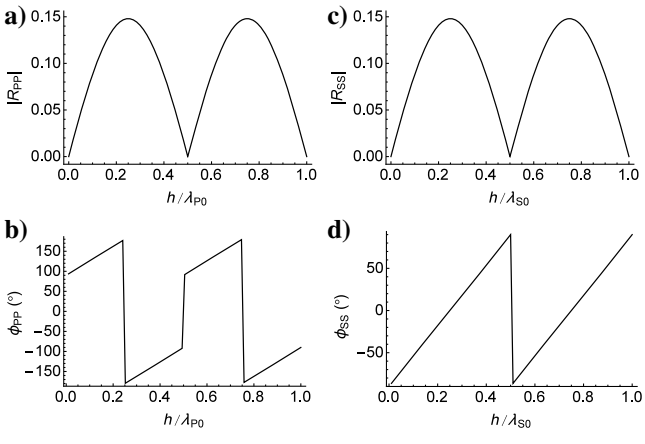

Figure 3. Similar to Figure 2, but for the low-velocity layer model. The vertical velocities in the layer are changed to $v_{P0}^{(M)} = 2.8$ km/s and $v_{S0}^{(M)} = 1.4$ km/s, whereas the other model parameters are the same as for the model in Figure 2.

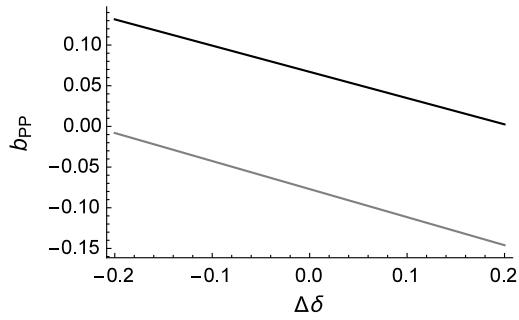

Figure 4. The dependence of the coefficient b_{PP} (equation B-2) on the change in the parameter δ across the layer boundaries. The black and gray lines correspond to the high- and low-velocity layer models, respectively. The medium parameters of both models are explained in the captions of Figures 2 and 3, respectively; only the parameter $\delta^{(M)}$ of the layer is changed to generate the dependence on $\Delta\delta$.

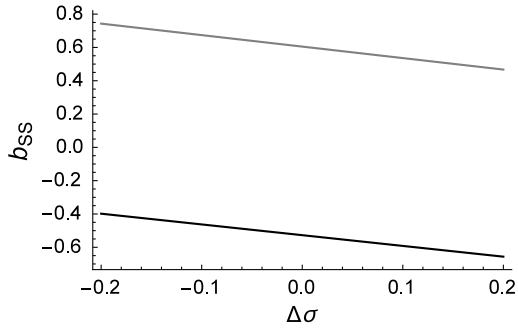

Figure 5. The dependence of the coefficient b_{SS} (equation B-8) on the change in the parameter σ across the layer boundaries. The black and gray lines correspond to the high- and low-velocity layer models, respectively. The high- and low-velocity layer models are explained in the captions of Figures 2 and 3, respectively; only the parameter $\delta^{(M)}$ is changed to generate the dependence on σ.

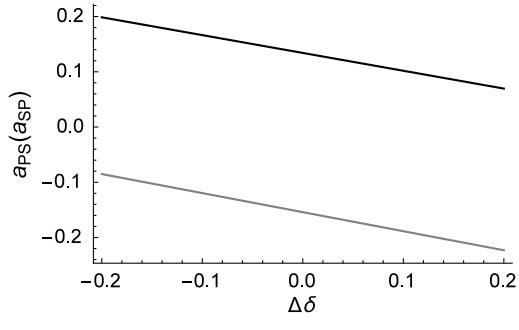

Figure 6. The dependence of coefficients a_{PS} (equation B-3) and a_{SP} (equation B-9) on the changes in the parameter δ across the layer boundaries. The black and gray lines correspond to the high- and low-velocity layer models, respectively. The high- and low-velocity models are explained in the captions of Figures 2 and 3, respectively.

shows that coefficient b_{SP} has an opposite dependence on the changes in parameters ε and δ across the layer boundaries. This implies that simultaneous increases or decreases in $\Delta\varepsilon$ and $\Delta\delta$ partially cancel each other out in coefficient b_{SP}.

In the third example, we test the accuracy of the approximate reflection coefficients (equations 29, 32, 35, and 38) for the low- and high-velocity layer models. The frequency of the incident waves is set to $f = 20$ Hz. Figures 9, 10, 11, and 12 show the angular variation of the reflection coefficients for subcritical incidence. All approximate coefficients generally reproduce the correct trend of the exact solutions. The phases of all the reflection coefficients vary with the incidence angle. The accuracy of the approximate P-P-wave reflection coefficient is generally acceptable, especially for the low-velocity model (Figure 11a). The angular variation of the magnitudes of the P-P- and SV-SV-wave reflection coefficients for the low-velocity model (Figures 11a and 12a) is more significant than those for the high-velocity model (Figures 9a and 10a). The magnitudes of the P-SV- and SV-P-wave reflection coefficients for the high-velocity model (Figures 9c and 10c) are generally much smaller than that for the low-velocity model (Figures 11c and 12c). Except for the approximate P-P reflection coefficient, all other approximations produce significant errors either in amplitude or phase, so they should not be applied to AVO inversion. Higher order expansions of the reflection coefficients with respect to the changes in the medium parameters across the layer boundaries may improve the accuracy of the solutions but would significantly increase their complexity.

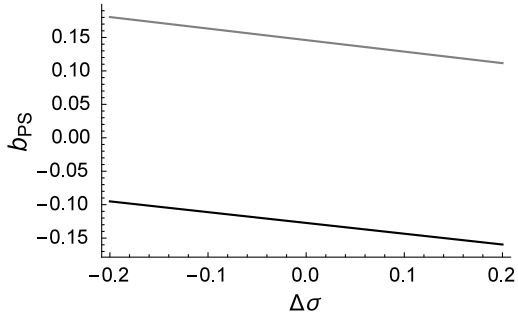

Figure 7. Similar to Figure 5, but for the coefficient b_{PS} (equation B-4).

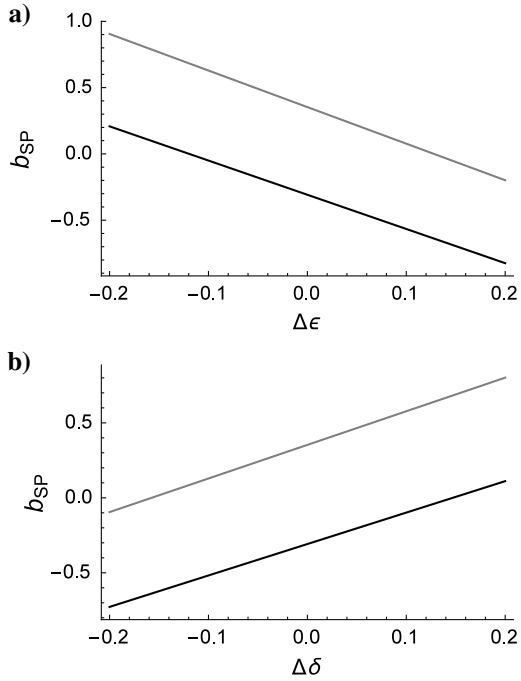

Figure 8. Variation of the coefficient b_{SP} (equation B-10) with the changes in the parameters (a) ε and (b) δ across the layer boundaries. The black and gray lines correspond to the high- and low-velocity layer models, respectively. The models are designed in a way similar to that explained in Figure 2, except that $\Delta\delta = 0$ and $\varepsilon^{(M)}$ is changed to obtain $\Delta\varepsilon$ in plot (a), whereas $\Delta\varepsilon = 0$ and $\delta^{(M)}$ is changed to obtain $\Delta\delta$ in plot (b).

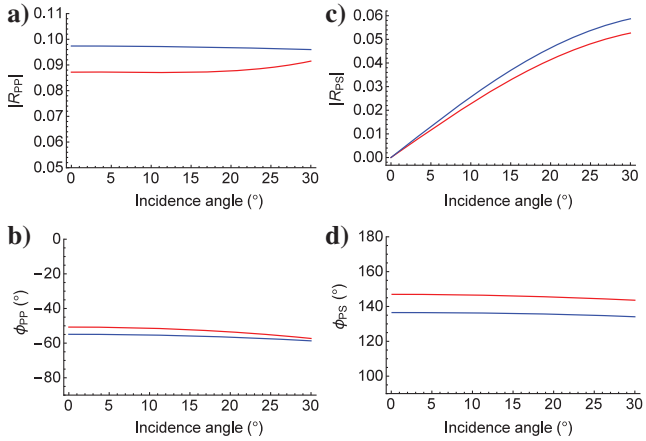

Figure 9. P-P- and P-SV-wave reflection coefficients for the high-velocity layer. The medium parameters are given in Figure 2. (a b) The magnitude and phase respectively of the P-P-wave reflection coefficient. (c d) The magnitude and phase respectively of the P-SV-wave reflection coefficient. The red and blue lines mark the exact and approximate solutions, respectively.

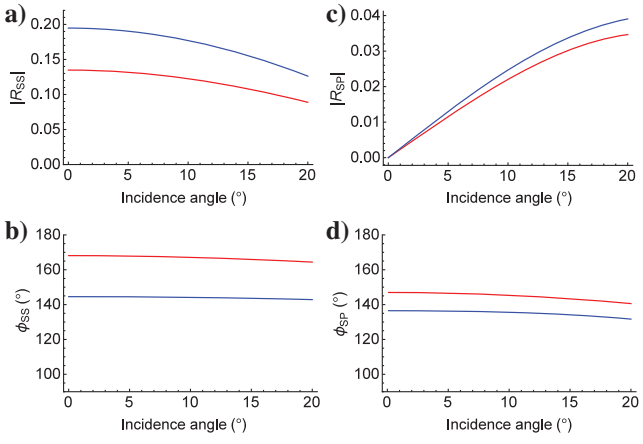

Figure 10. SV-SV- and SV-P-wave reflection coefficients for the high-velocity layer. The medium parameters are given in Figure 2. Plots (a and b) show the magnitude and phase, respectively, of the SV-SV-wave reflection coefficient. (c d) The magnitude and phase, respectively, of the SV-P-wave reflection coefficient. The red and blue lines mark the exact and approximate solutions, respectively.

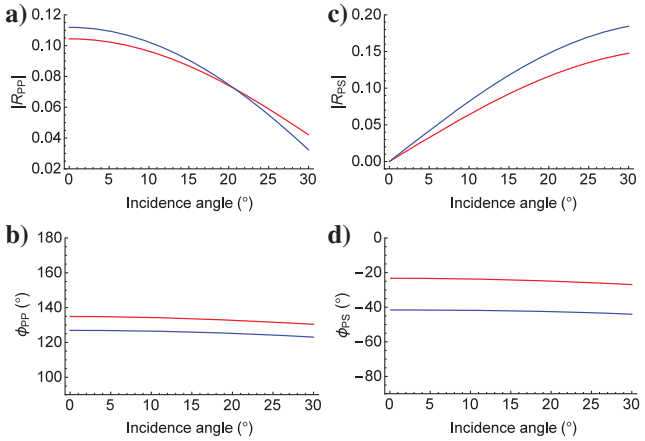

Figure 11. Similar to Figure 9, but for the low-velocity layer. The medium parameters are given in the captions of Figures 2 and 3.

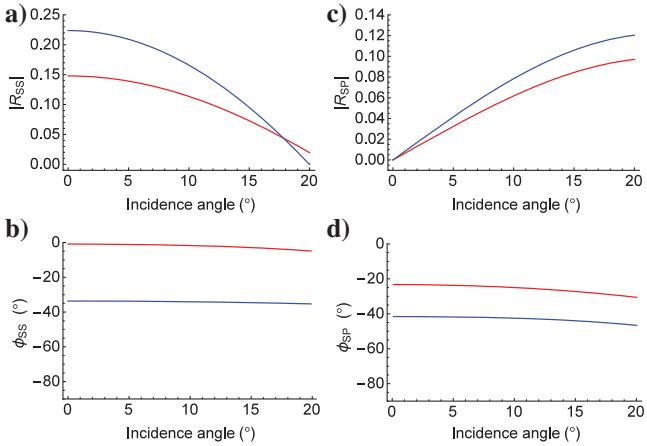

Figure 12. Similar to Figure 10, but for the low-velocity layer. The medium parameters are shown in the captions of Figures 2 and 3.

CONCLUSION

The exact reflection and transmission coefficients for a thin VTI layer embedded in a VTI medium are derived using the propagator matrix method. The exact normal-incidence reflection and transmission coefficients, expressed in terms of the impedances of the vertically propagating P- and SV-waves, are periodic functions of wavelength and frequency. The magnitudes of the P-P- and S-S-wave normal-incidence reflection coefficients have a similar dependence on layer thickness. The phase curve of the P-P-wave normal-incidence reflection coefficient for a low-velocity layer is similar to that of the S-S-wave coefficient from a high-velocity layer, and vice versa.

In the case of subcritical incidence, the approximate reflection coefficients are derived under the following assumptions: (1) the layer thickness is much smaller than the wavelength of P- and SV-waves inside the layer, (2) the contrasts in density and in the velocities of the vertically propagating P- and SV-waves are small, and (3) the layer and the background are weakly anisotropic.

The influence of transverse isotropy on the reflection coefficients from the layer is described in terms of the changes in the anisotropy parameters across the layer boundaries. The change in Thomsen's parameter δ across the layer boundaries determines the anisotropy contribution to the P-P-wave reflection coefficient, whereas the change in the anisotropy parameter σ contributes to the SV-SV-wave reflection coefficient. The change in δ across the layer boundaries has the same influence on the gradient term of the magnitudes of the P-SV- and SV-P-waves reflection coefficients. The change in σ across the layer boundaries contributes to the torsion term of the magnitude of the P-SV-wave reflection coefficients. The anisotropy contribution to the torsion terms of the SV-P-wave reflection coefficients is determined by the changes in ε and δ and cannot be expressed in terms of a single anisotropy coefficient.

Except for the approximate P-P-wave reflection coefficient, the other obtained approximations for the reflection coefficients are not accurate enough for quantitative AVO analysis or AVO inversion. However, they provide analytic insight into the behavior of the reflection coefficients and may qualitatively guide a numerical inversion based on the exact equations.

ACKNOWLEDGMENTS

We thank the Rock and Seismic (ROSE) Project for its support. The first author thanks V. Li, J. Cheng and an anonymous reviewer for their critical reviews, and especially thanks guest associate editor I. Tsvankin for the constructive review, many valuable suggestions, and improving the English of the paper.

APPENDIX A

PROPAGATOR MATRIX FOR A HORIZONTAL VTI LAYER

In this appendix, we adopt the method presented in Brekhovskikh (1980) to derive the propagator matrix for a horizontal VTI layer (Figure 1). The propagator matrix depends only on the layer parameters. For simplicity, we omit the superscript M, which is used to distinguish the layer from the upper and lower half-spaces, in the horizontal and vertical slowness components l and m and the vertical slowness component q. The in-plane wavefield inside the layer can always be represented by a superposition of upgoing and downgoing P- and SV-waves. We define the following particle displacement functions of these waves:

$$\mathbf{u}_{\mathrm{P}\downarrow} = A_{\mathrm{P}\downarrow}(l_{\mathrm{P}}, 0, m_{\mathrm{P}})^T \exp(-i\omega(t - px - q_{\mathrm{P}}z)), \quad \text{(A-1)}$$

$$\mathbf{u}_{\mathrm{S}\downarrow} = A_{\mathrm{S}\downarrow}(l_S, 0, -m_{\mathrm{S}})^T \exp(-i\omega(t - px - q_{\mathrm{S}}z)), \quad \text{(A-2)}$$

$$\mathbf{u}_{\mathrm{P}\uparrow} = A_{\mathrm{P}\uparrow}(l_{\mathrm{P}}, 0, -m_{\mathrm{P}})^T \exp(-i\omega(t - px + q_{\mathrm{P}}z)), \quad \text{(A-3)}$$

$$\mathbf{u}_{\mathrm{S}\uparrow} = A_{\mathrm{S}\uparrow}(l_S, 0, -m_{\mathrm{S}})^T \exp(-i\omega(t - px + q_{\mathrm{S}}z)), \quad \text{(A-4)}$$

where subscripts $\uparrow$ and $\downarrow$ denote the upgoing and downgoing waves, respectively, and subscripts P and S denote the P- and S-waves, respectively. The horizontal components of the unit polarization

vectors of these waves are chosen to be nonnegative, which agrees with the convention used in Aki and Richards (2002) to derive the reflection and transmission coefficients for an interface separating two isotropic half-spaces.

The total displacement inside the layer is given by

$$\mathbf{u} = \mathbf{u}_{P\downarrow} + \mathbf{u}_{S\downarrow} + \mathbf{u}_{P\uparrow} + \mathbf{u}_{S\uparrow}. \tag{A-5}$$

The components of the stress vector are expressed in terms of the displacement components (Graebner, 1992)

$$\tau_{zx} = c_{55}\left(\frac{\partial u_x}{\partial z} + \frac{\partial u_z}{\partial x}\right), \tag{A-6}$$

$$\tau_{zz} = c_{13}\frac{\partial u_x}{\partial x} + c_{33}\frac{\partial u_z}{\partial z}, \tag{A-7}$$

where τ_{zx} and τ_{zz} denote the horizontal and vertical components of the traction vector acting across a horizontal surface, and u_x and u_z denote the horizontal and vertical components of the particle displacement.

The displacements and tractions at the top and bottom of the layer are obtained by setting $z = 0$ and $z = h$ in equations A-5–A-7. As a result, we obtain eight linear equations involving the particle velocities and tractions at the top and bottom of the layer and the amplitudes of the upgoing and downgoing waves, where the particle velocity is the first-order derivative of the particle displacement with respect to time. Canceling the amplitudes of the upgoing and downgoing waves from these equations, we link the particle velocity and the traction at the bottom interface to the particle velocity and the traction at the top interface

$$\begin{pmatrix} v_x \\ v_z \\ \tau_{zz} \\ \tau_{zx} \end{pmatrix}\Bigg|_{z=0} = \begin{pmatrix} B_{11} & B_{12} & B_{13} & B_{14} \\ B_{21} & B_{22} & B_{23} & B_{24} \\ B_{31} & B_{32} & B_{33} & B_{34} \\ B_{41} & B_{42} & B_{43} & B_{44} \end{pmatrix} \begin{pmatrix} v_x \\ v_z \\ \tau_{zz} \\ \tau_{zx} \end{pmatrix}\Bigg|_{z=h}, \tag{A-8}$$

where v_x and v_z denote the horizontal and vertical components of the particle velocity, and B_{ij} is the transfer matrix. The elements B_{ij} are given by

$$B_{14} = i(l_P m_S \sin(hq_P\omega) + l_S m_P \sin(hq_S\omega))/(\xi c_{55}), \tag{A-9}$$

$$B_{23} = i(l_S m_P \sin(hq_P\omega) + l_P m_S \sin(hq_S\omega))/(\zeta c_{33}), \tag{A-10}$$

$$B_{32} = -i((c_{13}l_P p + c_{33}m_P q_P)(m_S p - l_S q_S)\sin(hq_P\omega) + (m_P p + l_P q_P)(c_{13}l_S p - c_{33}m_S q_S)\sin(hq_S\omega))/\xi, \tag{A-11}$$

$$B_{41} = -ic_{55}((m_P p + l_P q_P)(c_{13}l_S p - c_{33}m_S q_S)\sin(hq_P\omega) + (c_{13}l_P p + c_{33}m_P q_P)(m_S p - l_S q_S)\sin(hq_S\omega))/(\zeta c_{33}), \tag{A-12}$$

$$B_{31} = B_{42} = c_{55}(m_P p + l_P q_P)(m_S p - l_S q_S) \times (\cos(hq_P\omega) - \cos(hq_S\omega))/\xi, \tag{A-13}$$

$$B_{21} = B_{43} = -ic_{55}(l_S(m_P p + l_P q_P)\sin(hq_P\omega) + l_P(m_S p - l_S q_S)\sin(hq_S\omega))/(\zeta c_{33}), \tag{A-14}$$

$$B_{11} = B_{44} = (m_S(m_P p + l_P q_P)\cos(hq_P\omega) + m_P(-m_S p + l_S q_S)\cos(hq_S\omega))/\xi, \tag{A-15}$$

$$B_{13} = B_{24} = l_P l_S(-\cos(hq_P\omega) + \cos(hq_S\omega))/(\zeta c_{33}), \tag{A-16}$$

$$B_{22} = B_{33} = (m_P(-m_S p + l_S q_S)\cos(hq_P\omega) + m_S(m_P p + l_P q_P)\cos(hq_S\omega))/\xi, \tag{A-17}$$

$$B_{12} = B_{34} = i(l_P(m_S p - l_S q_S)\sin(hq_P\omega) + l_S(m_P p + l_P q_P)\sin(hq_S\omega))/\xi, \tag{A-18}$$

with

$$\xi = l_P m_S q_P + l_S m_P q_S, \zeta = l_S m_P q_P + l_P m_S q_S. \tag{A-19}$$

Assuming the layer to be thin and weakly anisotropic, we can expand B_{ij} with respect to $hq_P\omega$ and $hq_S\omega$ up to second order. Furthermore, q_P and q_S are approximated by their second-order series expansions with respect to the horizontal slowness p. Weak anisotropy approximation is also considered to derive simple approximation for B_{ij}. Finally, the approximation for B_{ij} is given by

$$\begin{pmatrix} B_{11} & B_{12} & B_{13} & B_{14} \\ B_{21} & B_{22} & B_{23} & B_{24} \\ B_{31} & B_{32} & B_{33} & B_{34} \\ B_{41} & B_{42} & B_{43} & B_{44} \end{pmatrix} \approx \begin{pmatrix} 1 & 0 & 0 & 0 \\ 0 & 1 & 0 & 0 \\ 0 & 0 & 1 & 0 \\ 0 & 0 & 0 & 1 \end{pmatrix} + ih\omega \begin{pmatrix} 0 & B_{12}^{(1)} & 0 & B_{14}^{(1)} \\ B_{21}^{(1)} & 0 & B_{23}^{(1)} & 0 \\ 0 & B_{32}^{(1)} & 0 & B_{34}^{(1)} \\ B_{41}^{(1)} & 0 & B_{43}^{(1)} & 0 \end{pmatrix} - h^2\omega^2 \begin{pmatrix} B_{11}^{(2)} & 0 & B_{13}^{(2)} & 0 \\ 0 & B_{22}^{(2)} & 0 & B_{24}^{(2)} \\ B_{31}^{(2)} & 0 & B_{33}^{(2)} & 0 \\ 0 & B_{42}^{(2)} & 0 & B_{44}^{(2)} \end{pmatrix}, \tag{A-20}$$

where

$$B_{21}^{(1)} = B_{43}^{(1)} = p((1 - 2r^2) + \delta), \tag{A-21}$$

$$B_{12}^{(1)} = B_{34}^{(1)} = p, \tag{A-22}$$

$$B_{14}^{(1)} = \frac{1}{\rho v_{S0}^2}, \tag{A-23}$$

$$B_{23}^{(1)} = \frac{1}{\rho v_{P0}^2}, \tag{A-24}$$

$$B_{32}^{(1)} = \rho, \tag{A-25}$$

$$B_{41}^{(1)} = \rho(1-4p^2v_{S0}^2(1-r^2)) + 2\delta\rho v_{P0}^2(1-2r^2)p^2 - 2\varepsilon\rho v_{P0}^2p^2, \tag{A-26}$$

$$B_{11}^{(2)} = B_{44}^{(2)} = \frac{1}{2}\left(\frac{1}{v_{S0}^2} - p^2(3-2r^2)\right) + \frac{\delta(2-3r^2)p^2}{2r^2} - \frac{\varepsilon p^2}{r^2}, \tag{A-27}$$

$$B_{13}^{(2)} = B_{24}^{(2)} = \frac{(1-r^2)p}{2\rho v_{S0}^2} + \frac{\delta p}{2\rho v_{S0}^2}, \tag{A-28}$$

$$B_{22}^{(2)} = B_{33}^{(2)} = \frac{1}{2}(1 + (1-2r^2)p^2) + \frac{\delta p^2}{2}, \tag{A-29}$$

$$B_{31}^{(2)} = B_{42}^{(2)} = (1-r^2)(1-2v_{S0}^2p^2)\rho p + \frac{1}{2}\delta\rho(1+2(1-2r^2)v_{P0}^2p^2)p - \varepsilon\rho v_{P0}^2p^3, \tag{A-30}$$

with

$$r = \frac{v_{S0}}{v_{P0}}, \tag{A-31}$$

where ε and δ are the Thomsen's (1986) parameters.

APPENDIX B

THE FUNCTIONS IN THE APPROXIMATE REFLECTION COEFFICIENTS

In this appendix, we give explicit expressions for the functions in the approximate reflection coefficients.

The functions a_{PP} and b_{PP} in equation 30 are given by

$$a_{PP} = -\frac{\Delta Z_P}{\bar{v}_{P0}\bar{Z}_P}, \tag{B-1}$$

$$b_{PP} = \frac{1}{\bar{v}_{P0}}\left(4\bar{r}^2\frac{\Delta G}{\bar{G}} - \frac{\Delta v_{P0}}{\bar{v}_{P0}} + \frac{\Delta Z_P}{2\bar{Z}_P} - \Delta\delta\right), \tag{B-2}$$

where $\bar{r} = \bar{v}_{S0}/\bar{v}_{P0}$ denotes the ratio between the velocities of the vertically propagating P- and S-waves, $\bar{Z}_{P0} = \bar{\rho}\bar{v}_{P0}$ denotes the P-wave impedance, and $\bar{G} = \bar{\rho}\bar{v}_{S0}^2$ denotes the shear modulus.

The functions a_{PS}, b_{PS}, c_{PS}, and d_{PS} in equations 33 and 34 are given by

$$a_{PS} = \frac{1+3\bar{r}+2\bar{r}^2}{2\bar{v}_{S0}}\frac{\Delta\rho}{\bar{\rho}} + \frac{2(1+\bar{r})}{\bar{v}_{P0}}\frac{\Delta v_{S0}}{\bar{v}_{S0}} - \frac{1}{2\bar{v}_{S0}}\Delta\delta, \tag{B-3}$$

$$\begin{aligned} b_{PS} &= -\frac{3+8\bar{r}+5\bar{r}^2}{4\bar{v}_{P0}}\frac{\Delta\rho}{\bar{\rho}} - \frac{1+4\bar{r}+3\bar{r}^2}{\bar{v}_{P0}}\frac{\Delta v_{S0}}{\bar{v}_{S0}} - \frac{1}{\bar{v}_{S0}}(\Delta\varepsilon - \Delta\delta), \\ &\approx -\frac{3+8\bar{r}+5\bar{r}^2}{4\bar{v}_{P0}}\frac{\Delta\rho}{\bar{\rho}} - \frac{1+4\bar{r}+3\bar{r}^2}{\bar{v}_{P0}}\frac{\Delta v_{S0}}{\bar{v}_{S0}} - \frac{\bar{r}^2}{\bar{v}_{S0}}\Delta\sigma, \end{aligned} \tag{B-4}$$

$$c_{PS} = \frac{(1+\bar{r})^2(1+2\bar{r})}{4\bar{v}_{S0}^2}\frac{\Delta\rho}{\bar{\rho}} + \frac{(1+\bar{r})^2}{\bar{v}_{P0}\bar{v}_{S0}}\frac{\Delta v_{S0}}{\bar{v}_{S0}} - \frac{1+\bar{r}}{4\bar{v}_{S0}^2}\Delta\delta, \tag{B-5}$$

$$d_{PS} = -\frac{(1+\bar{r})^2(4+7\bar{r})}{8\bar{v}_{P0}\bar{v}_{S0}}\frac{\Delta\rho}{\bar{\rho}} - \frac{(1+\bar{r})^2(1+4\bar{r})}{2\bar{v}_{P0}\bar{v}_{S0}}\frac{\Delta v_{S0}}{\bar{v}_{S0}} - \frac{1+\bar{r}}{2\bar{v}_{S0}^2}\Delta\varepsilon + \frac{4+5\bar{r}+\bar{r}^2}{8\bar{v}_{S0}^2}\Delta\delta, \tag{B-6}$$

where $\sigma \equiv (v_{P0}/v_{S0})^2(\varepsilon - \delta)$ is the combination of Thomsen's parameters primarily responsible for SV-wave propagation (Tsvankin, 2012, equation 1.67).

The functions a_{SS} and b_{SS} in equation 36 are given by

$$a_{SS} = \frac{1}{\bar{v}_{S0}}\left(\frac{\Delta G}{\bar{G}} - \frac{\Delta v_{S0}}{\bar{v}_{S0}}\right), \tag{B-7}$$

$$\begin{aligned} b_{SS} &= -\frac{1}{\bar{v}_{S0}}\left(\frac{9}{2}\frac{\Delta G}{\bar{G}} - \frac{3}{2}\frac{\Delta v_{S0}}{\bar{v}_{S0}} + \frac{1}{\bar{r}^2}(\Delta\varepsilon - \Delta\delta)\right), \\ &\approx -\frac{1}{\bar{v}_{S0}}\left(\frac{9}{2}\frac{\Delta G}{\bar{G}} - \frac{3}{2}\frac{\Delta v_{S0}}{\bar{v}_{S0}} + \Delta\sigma\right), \end{aligned} \tag{B-8}$$

where σ is defined after equation B-6.

The functions a_{SP}, b_{SP}, c_{SP}, and d_{SP} in equations 39 and 40 are given by

$$a_{SP} = a_{PS}, \tag{B-9}$$

$$b_{SP} = \frac{1}{\bar{v}_{P0}}\left(\frac{1-7\bar{r}^2-8\bar{r}^3-2\bar{r}^4}{4\bar{r}^3}\frac{\Delta\rho}{\bar{\rho}} - \frac{3+4\bar{r}+\bar{r}^2}{\bar{r}}\frac{\Delta v_{S0}}{\bar{v}_{S0}}\right) - \frac{1}{\bar{v}_{S0}}\left(\frac{1}{\bar{r}^2}\Delta\varepsilon - \frac{3+\bar{r}^2}{4\bar{r}^2}\Delta\delta\right), \tag{B-10}$$

$$c_{SP} = c_{PS}, \tag{B-11}$$

$$d_{SP} = \frac{(1+\bar{r})^2(1-2\bar{r}-8\bar{r}^2-2\bar{r}^3)}{8\bar{r}^2\bar{v}_{S0}^2}\frac{\Delta\rho}{\bar{\rho}} - \frac{(1+\bar{r})^2(4+\bar{r})}{2\bar{v}_{S0}^2}\frac{\Delta v_{S0}}{\bar{v}_{S0}} - \frac{1+\bar{r}}{2\bar{r}^2\bar{v}_{S0}^2}\Delta\varepsilon + \frac{3+4\bar{r}+2\bar{r}^2+\bar{r}^3}{8\bar{r}^2\bar{v}_{S0}^2}\Delta\delta, \tag{B-12}$$

where a_{PS} and c_{PS} are given in equations B-3 and B-5.

REFERENCES

Aki, K., and P. G. Richards, 2002, Quantitative seismology, 2nd ed.: University Science Books.

Brekhovskikh, L.M., 1980, Waves in layered media, 2nd ed.: Academic Press.

Brekhovskikh, L.M., and O. A. Godin, 1989, Acoustics of layered Media I: Plane and quasi-plane Waves: Springer.

Chapman, C., 2004, Fundamentals of seismic wave propagation: Cambridge University Press.

Fryer, G. J., and L. N. Frazer, 1984, Seismic waves in stratified anisotropic media: Geophysical Journal of the Royal Astronomical Society, **78**, 691–710, doi; doi: 10.1111/j.1365-246X.1984.tb05065.x.

Fryer, G. J., and L. N. Frazer, 1987, Seismic waves in stratified anisotropic media. II: Elastodynamic eigensolutions for some anisotropic systems: Geophysical Journal of the Royal Astronomical Society, **91**, 73–101, doi: 10.1111/j.1365-246X.1987.tb05214.x.

Graebner, M., 1992, Plane-wave reflection and transmission coefficients for a transversely isotropic solid: Geophysics, **57**, 1512–1519, doi: 10.1190/1.1443219.

Kennett, B. L. N., 1983, Seismic wave propagation in stratified media: Cambridge University Press.

Nayfeh, A.H., 1995, Wave propagation in layered anisotropic media: North-Holland.

Ursin, B., and G. U. Haugen, 1996, Weak-contrast approximation of the elastic scattering matrix in anisotropic media: Pure and Applied Geophysics, **148**, 685–714, doi: 10.1007/BF00874584.

Vavryčuk, V., 1999, Weak-contrast reflection/transmission coefficients in weakly anisotropic elastic media: P-wave incidence: Geophysical Journal International, **138**, 553–562, doi: 10.1046/j.1365-246X.1999.00890.x.

Vavryčuk, V., and I. Pšenčík, 1998, PP wave reflection coefficients in weakly anisotropic elastic media: Geophysics, **63**, 2129–2141, doi: 10.1190/1.1444506.

Rüger, A., 1996, Reflection coefficients and azimuthal AVO-analysis in anisotropic media: Ph.D thesis, Colorado School of Mines.

Rüger, A., 1997, P-wave reflection coefficients for transversely isotropic models with vertical and horizontal axis of symmetry: Geophysics, **62**, 713–722, doi: 10.1190/1.1444181.

Rüger, A., 1998, Variation of P-wave reflectivity with offset and azimuth in anisotropic media: Geophysics, **63**, 935–947, doi: 10.1190/1.1444405.

Thomsen, L., 1986, Weak elastic anisotropy: Geophysics, **51**, 1954–1966, doi: 10.1190/1.1442051.

Thomsen, L., 1993, Weak anisotropic reflections, *in* J. P. Castagna and M. M. Backus, eds., Offset dependent reflectivity: SEG.

Tsvankin, I., 2012, Seismic signatures and analysis of reflection data in anisotropic media, 3rd ed.: SEG.